Global Error Control of the Time-Propagation for the Schrödinger Equation with a Time-Dependent Hamiltonian

Katharina Kormann,* Sverker Holmgren,†
and Hans O. Karlsson‡

Abstract

We use a posteriori error estimation theory to derive a relation between local and global error in the propagation for the time-dependent Schrödinger equation. Based on this result, we design a class of h,p-adaptive Magnus–Lanczos propagators capable of controlling the global error of the time-stepping scheme by only solving the equation once. We provide results for models of several different small molecules including bounded and dissociative states, illustrating the efficiency and wide applicability of the new methods.

Key words global error control · h,p-adaptivity · Magnus–Lanczos propagator · time-dependent Schrödinger equation

1 Introduction

Understanding the dynamics of chemical reactions is a fundamental challenge in quantum chemistry. By exposing molecular systems to very short laser pulses it is possible to study, and also control, such reactions [37, 33, 24]. Mathematical models of dynamic quantum mechanical processes, e.g., in chemical reactions, are based on the time-dependent Schrödinger equation (TDSE). For realistic problems, this equation cannot be solved analytically, and numerical solution methods are of great importance to interpret experimental studies and to provide a deeper theoretical understanding of the reaction dynamics.

For problems including time-dependent fields, e.g., describing collisions or interaction with electromagnetic radiation, the Hamiltonian operator in the

*Division of Scientific Computing, Department of Information Technology, Sweden. Graduate School in Mathematics and Computing (FMB).

†Division of Scientific Computing, Department of Information Technology, Uppsala University, Sweden.

‡Quantum Chemistry, Department of Physical and Analytical Chemistry, Sweden. Uppsala Multidisciplinary Center for Advanced Computational Science (UPPMAX).

TDSE depends explicitly on time. For highly accurate simulations involving such Hamiltonians, the temporal variation has to be resolved by the time-propagation scheme [19]. For such problems, it can be assumed that a time-propagation method that includes automatic step size control can be more efficient and simpler to use. It is also desirable to have an a posteriori estimate of the error, resulting in a scheme where the step size is chosen to control (some functional of) the *global* error introduced by the time propagation. Interesting properties to control can be the ℓ_2 error of the computed wave function or a cross-correlation function of interest (i.e., the scalar product of the computed wave function with some given state of the molecule).

An overview of standard propagation techniques for the TDSE with a time-dependent Hamiltonian is given in [21]. A suitable numerical integrator for the TDSE should preferably preserve the most important physical properties of the exact propagator — unitarity and time-reversibility. In [19], integrators with these properties based on two approaches are discussed; exponential integrators and symplectic integrators based on partitioned Runge–Kutta (PRK) formulas. For the PRK methods, symplecticity guarantees unitarity of the evolution operator (cf. [8]). As demonstrated, e.g., in [30], symplecticity is lost if step size control in a straightforward way is applied. Therefore, we focus on adaptivity for exponential integrators in this paper, where at least unitarity can easily be retained in a practical implementation.

In [5], Cao and Petzold introduce a posteriori estimates based on the adjoint method for systems of ordinary differential equations (ODE). Similar techniques are also available for PDEs within the FEM framework, see, e.g., [2, 6] and references therein. In this paper, we show how the theory developed in [5] can be applied to the TDSE after spatial discretization by the method of lines,

$$\begin{aligned} \mathrm{i}\hbar\frac{d}{dt}\psi(t) &= H(t)\psi(t), \\ \psi(0) &= \psi_0. \end{aligned} \tag{1}$$

Here, $\psi(t)$ is the vector of the values of the wave function at time t representing the spatial degrees of freedom and H is the Hamiltonian matrix which is hermitian in the mathematical model of the physical process. Note that this model is posed on an unbounded domain which is infeasible for numerical computations. For bound states, the wave function will stay within certain bounds and the domain can be truncated and, e.g., periodic boundary conditions can be imposed. For such problems, hermiticity is maintained. For dissociative states, however, we normally have to include a transparent boundary resulting in that hermiticity is lost.

In this paper, we only discuss time-discretization techniques and consider (1) as a system of ODE. We assume that we have projected he spatial part of the problem onto a subspace that is sufficient to obtain the desired accuracy. A suitable grid can, for instance, be determined using Fourier analysis [16]. In this

case, the Hamiltonian matrix, corresponding to the unbounded operator in the continuous case, is bounded (but may have a large norm).

Based on the a posteriori estimate, we derive an h,p-adaptive Magnus–Lanczos time-propagator with global error control. We show that, due to the conservation of probability and time-reversibility of the TDSE, an estimate of the global error can be achieved without explicitly solving the adjoint problem.

The outline of this paper is as follows. In the next section, we investigate the connection between local and global error for the TDSE and derive a low-cost error estimator. Sec. 3 discusses the truncated Magnus expansion as a tool for numerical integration, with a focus on the local error of this propagator. We then use these results to design an adaptive Magnus–Lanczos propagator allowing for global error control in Sec. 4. The performance of the proposed algorithm is demonstrated in Sec. 5 for one-dimensional models of laser excitation of the rubidium dimer (Rb_2), the iodine-bromide molecule (IBr), and a three-dimensional model of a chlorine dioxide (ClO_2) molecule[1]. Sec. 6 addresses the question in which cases it is preferable to solve the dual problem anyway, and Sec. 7 concludes the article.

2 Error Growth in the TDSE: From Local to Global Error

A simple adaptive method is often based on local error estimates that can easily be derived, computed, and used for controlling the step size in an individual step. For example, there is a vast literature on step size control for Runge–Kutta methods using two embedded methods to estimate the local error (see, e.g., [12]). Raptis and Cash [28] exemplify how these techniques can be applied to the one-dimensional TDSE. However, in many settings it is more interesting to bound the *global* error, i.e., computing the desired quantity at a final time within a given accuracy bound. In this section, we study how local perturbations influence the error in the solution of the TDSE (and other PDEs with the same conservation properties).

2.1 Error growth

We first consider the general linear system of ODE

$$\begin{aligned} \dot{y}(t) &= A(t)\,y(t), \\ y(0) &= y_0. \end{aligned} \tag{2}$$

Assume that we integrate this system over the interval $[0,T]$, and let $0 = t_0 \le \ldots \le t_k \le \ldots \le t_M = T$ denote the discrete points in time where the numerical method evaluates approximations y_k of $y(t_k)$. Also, let $h_k = t_k - t_{k-1}$ denote the time steps and let $h = \max(h_k)$.

[1] Note that the alternative notation OClO is common in the chemical literature to account for the structure of the molecule.

We are interested in estimating (some functional of) the global error,

$$e(T) = y(T) - y_M.$$

As remarked earlier, Cao and Petzold [5] have shown how to connect the global and local errors for step size control in ODE solvers by using the adjoint problem. We begin by briefly reviewing their work.

Let $\widehat{y}$ be the solution of the perturbed ODE

$$\begin{aligned} \dot{\widehat{y}}(t) &= A(t)\widehat{y}(t) + r(t), \\ \widehat{y}(0) &= y_0 + R, \end{aligned}$$

where $\widehat{y}$ represents an interpolant of the numerical solution.

A functional $z^H e(T)$ of the error (where z is normalized) can be calculated using

$$z^H e(T) = \int_0^T \lambda^H(s) r(s)\, ds + \lambda^H(0) R, \tag{3}$$

where λ solves the adjoint problem

$$\begin{aligned} \dot{\lambda}(t) &= -A^H(t)\lambda(t) \\ \lambda(T) &= z. \end{aligned}$$

In this paper, we apply this theory to the semi-discretized time-dependent Schrödinger equation (1). For this equation, we have that $A = -iH$, and, if the Hamiltonian matrix H is hermitian, the dual equation is identical to the primal. We then also know that the ℓ_2 norm of λ is preserved. This can be exploited to simlify (3). Firstly, we apply the Cauchy–Schwarz inequality,

$$|z^H e(T)| \le \int_0^T \|\lambda(t)\|\, \|r(t)\|\, dt + \|\lambda(0)\|\, \|R\|.$$

Then, norm-conservation gives

$$|z^H e(T)| \le \int_0^T \|r(t)\|\, dt + \|R\|. \tag{4}$$

Since the bound (4) is independent of z, it yields an estimate for any functional of the error. In particular, the choice $z = \frac{e(T)}{\|e(T)\|}$ results in an estimate for $\|e(T)\|$. From (4), it is also clear that the temporal error induced by the numerical propagator can be bounded by a term that increases linearly in T. Moreover, an error in the initial wave function is neither damped nor increased as time evolves.

Remark. If we want to extend the error estimate to the spatial discretization, it is interesting to note that the error in the function evaluation in the ODE (e.g., from the computation of the spatial derivative in the TDSE) can likewise be bounded by a term that increases linearly in T.

In contrast to the general case discussed in [5], the estimate (4) does not require solving the adjoint problem. This reduces the cost of global error control significantly. However, using (4) potentially results in that the error is overestimated and that unnecessarily small steps are used. We will investigate this further in Sec. 6. Also note that if we are interested in the norm of the error, the vector z depends on the solution and is thus unknown. In this case, we first have to determine suitable values of z, for instance by the small sample statistical method [18]. This is avoided by using our estimate (4), again reducing the cost and also increasing the reliability of the global error control.

2.2 An efficient global error estimate for the TDSE

In the previous section, we described how a perturbation of the Hamiltonian matrix and the initial data, e.g., arising from the numerical approximation, influences the global error. As a next step, we estimate these perturbations. For the general system (2), Cao and Petzold derive an estimate for multi-step methods with reference to Gear [7] for one-step methods.

In the following, we demonstrate how to distribute the errors coming from the individual time steps in order to be able to get an efficient estimate by only applying local information to estimate the global perturbation. Consider the time step from t_{k-1} to t_k as the solution of the perturbed initial-value problem

$$\begin{aligned}\dot{\widehat{\psi}}(t) &= -\mathrm{i}H(t)\widehat{\psi}(t) + r_k(t)\\ \widehat{\psi}(t_{k-1}) &= \psi_{k-1} = \psi(t_{k-1}) + R_{k-1},\end{aligned}$$

where r_k is the residual due to the numerical approximation in the present step and R_{k-1} is the error made in the preceding steps.

Using (4), it holds that

$$\|e(t_k)\| \le \int_{t_{k-1}}^{t_k} \|r_k(t)\|\,\mathrm{d}t + \|R_{k-1}\|.$$

Thus the error in the initial value for the next time step, from t_k to t_{k+1}, can be estimated by $\|R_k\| = \|e(t_k)\|$. This leads to a recursion which results in the following estimate of the global error

$$\|e(T)\| \le \sum_{k=1}^{M} \int_{t_{k-1}}^{t_k} \|r_k(t)\|\,\mathrm{d}t + \|R_0\|. \tag{5}$$

If we now prescribe that $\frac{1}{h_k}\int_{t_{k-1}}^{t_k} \|r_k(t)\|\,dt \le \frac{\varepsilon}{T}$, i.e., that the error of time step k should not exceed the fraction h_k/T of the allowed global error, and assume that the initial value $\psi(0)$ is given correctly, it follows that

$$\|e(T)\| \le \frac{\varepsilon}{T}\sum_{k=1}^{M} h_k \le \varepsilon.$$

Thus we have found a way to control the global error based on a estimate of the error of the numerical integrator in each single step.

Assume that we can estimate the local error e_k^{loc} for time step k. Then we can view this error as perturbation of the initial value for the problem on the next time interval and, from the results of the previous section on how local errors are transported, we have that

$$\|e(T)\| \leq \sum_{l=1}^{M} \left\| e_k^{\text{loc}} \right\|.$$

It remains now to find a way of how to compute the local perturbations r_k. As will be shown in Sec. 3.1 below, this quantity can be estimated quite easily for the Magnus propagator.

2.3 Generalization for problems with transparent boundary conditions

So far, we have assumed that the Hamiltonian in the TDSE (1) is Hermitian. However, if the problem setting involves a dissociative state, we have to truncate the computational domain in space and introduce a non-reflecting boundary condition to model the infinite domain. There are two techniques commonly used for this, perfectly matched layers (PML) [11] (which is closely related to complex scaling as Hein *et al.* [13] point out), and complex absorbing potentials (CAP) [22]. Both approaches introduce artificial damping which results in that the Hamiltonian matrix is not Hermitian.

For a TDSE problem with dissociative states, the sign of the complex absorbing potential and the sign of the transformation to complex coordinates changes in the dual problem, resulting in that the dual and primal equations are not equal. However, since the dual problem is solved backwards in time, the wave-packet for this problem is also damped. This means that the norm of the dual solution λ is on longer conserved but

$$\|\lambda\| \leq 1. \tag{6}$$

This means the estimate (5) derived above is still valid, but it might be less strict. However, note that the adjoint problem is solved backward in time. Let us suppose that the target ϕ is concentrated on the computational domain. If the wave-packet dissociated, this would then mean that a dissociated state would move together again. Apart from numerical perturbations, we can thus assume that the norm of the dual problem is still conserved, that is, $\|\lambda\| \approx 1$.

3 Truncating the Magnus Expansion

In this section, we introduce the truncated Magnus expansion [17] over a small time interval as a tool for designing a numerical propagator and investigate the

truncation error. We combine this knowledge of the local behavior with the results from the preceding section to derive an estimate of the global error.

3.1 The Magnus propagator

For problems with a *time-independent* Hamiltonian, the solution of the TDSE (1) can be given in analytical form,

$$\begin{aligned} \psi(t_k) &= U(t_{k-1}, t_k)\psi(t_{k-1}) \\ U(t_{k-1}, t_k) &= \exp\left(-\frac{\mathrm{i}h_k}{\hbar}H\right). \end{aligned}$$

For *time-dependent* Hamiltonians, the Magnus expansion provides an analytical representation of the evolution operator where the higher order terms decrease in powers of h_k [17]. This representation can be used as a basis for the numerical integration of the TDSE (1) in case a sufficiently small time step h_k is chosen and the solution is propagated by an exponential integrator based on a truncated Magnus expansion. This procedure is successively repeated until the solution at the desired time is reached.

The design of Magnus-based propagators involves two steps: Truncating the Magnus expansion in a suitable way, and computing the matrix exponential efficiently. We will consider the first step below and postpone the second to Sec. 4.1.

Since the terms of the Magnus expansion contain an increasing number of commutators, evaluating them becomes costly as the order is increased. Several ways of reducing the computational complexity have been proposed. In [3], the terms are rearranged and in [4] the matrix exponential is split and a fourth-order commutator-free scheme is derived. Starting from the formulation in [3], we have earlier shown that it is often possible to simplify the evaluation of the truncated Magnus expansion even further for the TDSE by evaluating some of the terms simplifying [19].

3.2 Truncating the Magnus expansion: Local error

We first note that a Magnus-based propagator can be reformulated as a one-step method using the definition of the matrix exponential,

$$\exp A = \sum_{l=0}^{\infty} \frac{A^l}{l!} = I + \sum_{l=1}^{\infty} \frac{A^l}{l!}.$$

This representation is not useful for practical computations, but it shows that the perturbed problem can be theoretically constructed as in [7] for one-step methods. In the following, we develop a more practical strategy.

Consider the linear differential equation

$$\dot{\psi}(t) = A(t)\psi(t) \tag{7}$$

with $A(t) = -\frac{\mathrm{i}}{\hbar}H(t)$. The Magnus expansion is an expression $\Omega(t)$ such that the solution of (7) can be written in the form (cf. [17])

$$\psi(t) = \exp(\Omega(t))\psi_0. \tag{8}$$

The relation between $A(t)$ and $\Omega(t)$ is given by

$$A(t) = \mathrm{dexp}_{\Omega(t)}(\dot{\Omega}(t)),$$

where the dexp operator is defined by

$$\mathrm{dexp}_B(C) = \sum_{l\geq 0} \frac{1}{(l+1)!}\mathrm{ad}_B^l(C),$$

with $\mathrm{ad}_B(C) = [B,C]$ and $\mathrm{ad}_B^l(C) = \mathrm{ad}_B(\mathrm{ad}_B^{l-1}(C))$. If the step length h is sufficiently small, the dexp operator can be inverted and the Magnus expansion gives an expression for Ω,

$$\Omega(t) = \sum_{l\geq 0} \theta_l. \tag{9}$$

The terms in θ_l are built up of l nested commutators and $l+1$ integrals and decay as $\theta_l = \mathcal{O}(h^{l+2})$ for $l > 0$. For a numerical solution, we truncate the expansion,

$$\Omega^{[n]} = \sum_{l=0}^{n-2} \theta_l.$$

The numerical solution then solves the perturbed equation

$$\dot{\widetilde{\psi}}(t) = A^{[n]}\widetilde{\psi}, \tag{10}$$

with $A^{[n]}(t) = \mathrm{dexp}_{\Omega^{[n]}(t)}(\dot{\Omega}^{[n]}(t)) = A(t) + r$ and $r \in \mathcal{O}(h^n)$. Using the fact that $\mathrm{dexp}_B(C) = f(\mathrm{ad}_B)(C)$ with $f(z) = (\mathrm{e}^z - 1)/z$, we can rewrite the residual as

$$\rho_n(\mathrm{ad}_{\Omega^{[n]}}(\mathrm{ad}_\Omega^{p-1}(B)),$$

(with ρ_n being the nth remainder term in the Taylor expansion of f) plus the non-vanashing part of the first $n-1$ terms of the expansion $\mathrm{dexp}_{\Omega^{[n]}(t)}(\dot{\Omega}^{[n]}(t))$. For a numerical estimation of the residual, we are interested in having an easy-to-compute approximation to the non-vanishing residual. Therefore, we only take the leading order term $\dot{\theta}_{n-1}$.

Knowing the residual, we can compute the local error in time step k,

$$\begin{aligned} e_k^{\mathrm{loc}} &= \int_{t_{k-1}}^{t_k} r(\tau)\widetilde{\psi}_k(\tau)d\tau = \int_{t_{k-1}}^{t_k} \dot{\theta}_{n-1}(\tau)\widetilde{\psi}_k(\tau)\,d\tau + \mathcal{O}(h^{n+2}) \\ &= \theta_{n-1}(t_k)\widetilde{\psi}(\xi) + \mathcal{O}(h^{n+2}), \end{aligned}$$

for some $\xi \in [t_{k-1}, t_k]$. The ℓ_2 norm of the local error can then be estimated by

$$\left\| e_k^{\mathrm{loc}} \right\| = \left\| \theta_{n-1}(t_k)\widetilde{\psi}(\xi) \right\| + \mathcal{O}(h^{n+2}). \tag{11}$$

This gives an expression for the local error under the assumption that the Magnus expansion convergences. The classical proof of the convergence of the Magnus expansion for ODE systems is based on the assumption $\int_{t_{k-1}}^{t_k} \|A(\xi)\|_2 \, d\xi < \pi$, i.e., in essence, $h \cdot \|A(t)\|$ has to be small (cf. [23]). For the continuous Schrödinger equation, where the Hamiltonian operator is unbounded, the classical result is insufficient. Hochbruck and Lubich [14] explain, however, how to obtain error bounds without requiring convergence in the expansion.

We briefly review their reasoning and discuss how this is related to our algorithm. In [14], the case

$$A(t) = -\mathrm{i}H(t) = -\mathrm{i}(W + V(t)) \tag{12}$$

is considered, where $W = -\Delta + I$ and $\|\frac{d^m}{dt^m} V(t)\| \leq M_m$, $m = 0, 1, 2, \ldots$.

For this Hamiltonian and a space discretization with the pseudo-spectral method, commutator bounds of the type

$$\|[A(\tau_l), [\ldots, [A(\tau_1), A(\tau_0)]]\ldots] \, v\| \leq K h \|W^{l/2} v\| \tag{13}$$

can be proven.

Under the additional assumption that $h\|W^{1/2}\| \leq c$ for some constant c, the remainder of a nth order Magnus expansion is thus bounded by

$$\|r \, v\| \leq C h^n \|W^{(n-1)/2} v\|. \tag{14}$$

Since $\|W^{1/2}\| \propto \frac{1}{\Delta x}$, these results show that care has to be taken when considering the residual. Including Δx in the estimate for the local error, we have

$$\|e_k^{\mathrm{loc}}\| = \|\theta_{n-1}(t_k)\widetilde{\psi}(\xi)\| + \mathscr{O}\left(\frac{h^{n+2}}{(\Delta x)^n}\right),$$
$$\|\theta_{n-1}(t_k)\widetilde{\psi}(\xi)\| = \mathscr{O}\left(\frac{h^{n+1}}{(\Delta x)^{n-1}}\right).$$

In this paper, we are only interested in bounding the error in time given a fixed discretization in space. That is to say, we do not consider the whole solution space of the Hamiltonian operator but first project onto a subspace of interest. For this case $(\Delta x)^{-1}$ remains bounded. Nevertheless, relaxing the assumption $\int_{t_{k-1}}^{t_k} \|A(\xi)\|_2 \, d\xi < \pi$ as provided by the results in [14] is desirable since the constants that are proportional to some power of $(\Delta x)^{-1}$ can be very large. In our experiments, we choose the step size only regarding accuracy requirements and do not observe any problems with stability, even if the Hamiltonians that we consider are more complicated than those of form (12) (which is why the results by Hochbruck and Lubich do not directly apply to our situation).

Note that Wensch *et al.* [35] derived a locally adaptive Magnus propagator. Their reasoning is based on extrapolation and does not take the difficulties with the norm of the Hamiltonian into account (i.e., they rely on convergence of the Magnus expansion). The resulting error indicator is similar to ours but includes an additional higher-order term.

3.3 Global error control

In Sec. 2, we have shown that a global error smaller than some tolerance ε can be achieved by controlling the local error. If the numerical solution ψ_{k-1} has been computed, the next step size h_k should be chosen such that the local error weighted by the step length is smaller than $\frac{\varepsilon}{T}$.

As discussed in the previous section, a first order estimate of the error is given by (11). In this estimate, the value of ξ is unknown. Since $\widetilde{\psi}$ varies only of the order h over the interval, it is sufficient to use $\widetilde{\psi}_{k-1}$ for getting a first order estimate.

The adaptive method should hence approve a step if

$$\frac{1}{h_k}\|\theta_{n-1}(t_{k-1}+h_k))\psi_{k-1}\| \leq \frac{\varepsilon}{T}. \tag{15}$$

The only unknown in (15) is the step size h_k. However, the left hand side is still nonlinear in this parameter and it would be too costly to solve this equation exactly. To resolve this issue, we use that the error is of order h_k^{n+1}. We then solve equation (15) by the fixed point iteration

$$s_0 = h_{k-1}, \qquad s_{j+1} = \left(s_j \frac{\varepsilon/T}{\|\theta_{n-1}(t_{k-1}+s_j))\psi_{k-1}\|}\right)^{\frac{1}{n}} \cdot s_j. \tag{16}$$

We iterate until $\frac{1}{s_J}\|\theta_{n-1}(t_{k-1}+s_J))\psi_{k-1}\| \leq \frac{\varepsilon}{T}$ and then set $h_k = s_J$. In order to make the step size control more robust, one can check, after advancing the solution to time level k, if $\frac{1}{h_k}\|\theta_{n-1}(t_{k-1}+h_k))\psi_k\| \leq \frac{\varepsilon}{T}$. We also include safety factors in (16) to keep the number of iterations and dismissed steps small.

When using the commutator-reduced formulation from [3] where each odd term is merged with the following even term, we replace θ_{n-1} by $\tilde{\theta}_{n-1} = \theta_{n-1}+\theta_n$.

4 A Magnus–Lanczos-Propagator with Global Error Control

So far, we have only discussed the truncation of the Magnus expansion. However, using a Magnus-based numerical integrator requires repeatedly calculating matrix exponentials. A direct computation involving complete diagonalization is far too expensive for large systems. If the discrete Hamiltonian is symmetric, the Lanczos algorithm is a viable alternative [26].

4.1 Short-iterative Lanczos propagator

The Lanczos algorithm computes the matrix exponential applied to a vector, $\exp(-\frac{\mathrm{i}h_k}{\hbar}\Omega^{[n]})\psi_k$, using a polynomial expansion (see, e.g., [15]). The process successively creates an orthonormal basis in the pth order Krylov subspace spanned by $\{\psi, \Omega^{[n]}\psi, (\Omega^{[n]})^2\psi, \ldots, (\Omega^{[n]})^{p-1}\psi\}$. The approximative solution is then given by the projection of the exact solution onto the Krylov subspace.

The Lanczos algorithm converges superlinear after a certain number of iterations — depending in particular on the time step h_k in our case. It turns out that for practical solution of the TDSE, the algorithm is most efficient for p of the order of ten [32]. The parameter p has to be chosen larger when h_k is increased because the wave function from the previous time step is used as the initial vector for the Lanczos iteration. This means that a relatively small time step should be used, but this is required anyway when the Hamiltonian has an intense time-dependence.

Given the time step h_k, we have to decide how large we want to choose the Krylov space. Y. Saad [29] and Hochbruck *et al.* [15] propose to stop the Lanczos iterations as soon as the generalized residuum is small enough. For the TDSE, the corresponding termination criterion is

$$\Delta t \left| \left(\exp(-\mathrm{i}/\hbar \Delta t \Omega_p^{[n]}) \right)_{p,1} \right| (\Omega_{p+1}^{[n]})_{p+1,p} < \mathrm{tol}, \tag{17}$$

where $\Omega_p^{[n]}$ is the approximation of the Magnus-weighted Hamiltonian $\Omega^{[n]}$ in the p-dimensional Krylov space. Here, the notation $(A)_{i,j}$ is used for the (i,j)-entry of the matrix A.

4.2 Adaptivity

Gathering the results in the previous sections, we have three parameters at hand that can be chosen adaptively when performing a time step: The time step h_k, the order n of the truncated Magnus series, and the order p of the Krylov space. Since varying all these parameters at the same time is difficult, we simplify the procedure using a few reasonable assumptions: First, we assume that we have a significant time-dependence in the Hamiltonian. Otherwise all terms in the Magnus expansion but the first will vanish. In that case, the propagation problem would simplify a lot, and other more efficient time-marching methods are available (cf. [20]). Next, we also decide to fix the order of the Magnus expansion n at some low order instead of adaptively choosing this parameter. The reason for this is that higher order Magnus terms get increasingly complicated and costly to evaluate. The actual choice of n depends on the structure of the problem and should assure that the commutators involved are not too expensive to evaluate. As we will see later, $n = 2, 4$ are convenient choices in many common applications.

In Sec. 3.3, we proposed to use relation (15) to choose the step size h_k based on the Magnus approximation. This approach can easily be combined with a p-adaptive Lanczos method, i.e., relation (17). We found this combination of an h-adaptive Magnus and a p-adaptive Lanczos method to be very attractive. For the time steps chosen by the Magnus approximation the number of Lanczos iterations necessary to keep the accuracy is rather small and thus the Lanczos iteration is efficient. By imposing some upper bound on the time step, convergence

of the Lanczos method is assured also for situations where the time-dependence of the Hamiltonian is weak.

5 Experiments: Light-Matter Interaction

To examine the performance of the new adaptive time-propagation algorithms, we apply the Magnus–Lanczos algorithm with global error control to TDSE models describing optical excitation of molecules using, e.g., laser pulses. We first consider a basic model that includes two electronic states and discuss the corresponding Magnus expansion. Fig. 1 shows a generic configuration. In this basic model, the TDSE has the form

$$H = \begin{pmatrix} T_{\text{kin}} + V_g(x) & V_c(t) \\ V_c(t) & T_{\text{kin}} + V_e(x) \end{pmatrix}, \tag{18}$$

where wave packets are propagated on two potential energy surfaces $V_{g/e}$, coupled via a time-dependent term $V_c(t)$. As mentioned earlier, we will present computational results for three different molecules, Rb_2, ClO_2, and IBr. The simulations for the one-dimensional Rb_2 model demonstrate the efficiency of our new adaptive M/L methods for different orders of accuracy. This model is also used later for providing a comparison of our low-cost algorithm for global error control with a more standard version where the dual problem is actually solved. The three-dimensional ClO_2 model is used to verify that our new schemes are applicable also to problems with several spatial degrees of freedom. Finally, we provide computational results for the IBr system, where also a third, dissociative state is included. This example shows that the method can also be applied for problems where the Hamiltonian matrix is non-hermitian.

In our examples, we model experiments where the electronic states are coupled with an ultra-fast pulse, $V(t) = \mu_{ge}(r)\varepsilon(t)$, where the light-matter interaction is treated semi-classically, i.e., $\varepsilon(t) = E_0 \cdot \exp\left(-\frac{1}{2}\left(\frac{t-t_0^2}{\sigma}\right)^2\right) \cdot \cos(\omega(t-t_0))$. Also, we assume that the Condon approximation is used, i.e., the transition dipole moment μ_{ge} is constant.

As remarked earlier, we discretize the kinetic energy operator using a pseudospectral method on a uniform grid in space, resulting in that the action of the kinetic energy matrix is easily computed using an FFT/IFFT pair. Since this is the most costly part of the numerical propagation, we count the number of such pairs needed in each simulation compare the computational costs for different methods. Note that for each multiplication by the Hamiltonian matrix (18), one FFT/IFFT pair for each state is needed.

For determining the error for the numerical schemes, we compare the results to a reference solution, computed using a very small, uniform time step.

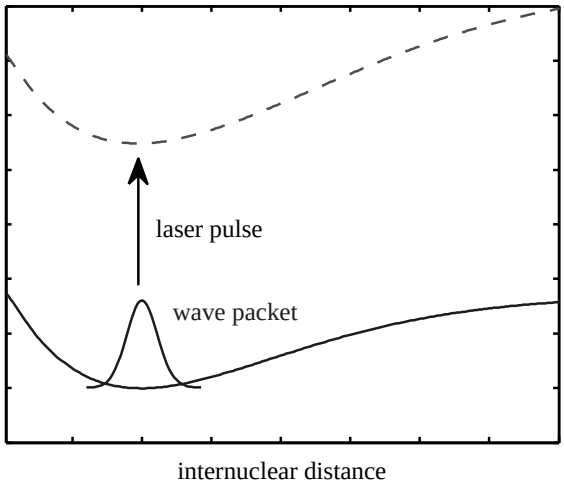

Figure 1: Configuration of a system with two electronic states: The wave packet is initially concentrated in the ground state (—) that is coupled to an excited state (– –) by a laser field.

5.1 Magnus–Lanczos propagators for a two-state system

Before presenting the simulations, we give some more details about the propagator for system (18). For a system with a Hamiltonian given by (18) one can simplify the first two Magnus terms by analytically computing the commutators [19] yielding the following fourth order truncation

$$\begin{aligned}\Omega^{[4]}(t_{n+1},t_n) = &-\frac{\mathrm{i}}{\hbar}\cdot\Delta t\cdot\begin{bmatrix} T_{\mathrm{kin}}+V_a & C_0 \\ C_0 & T_{\mathrm{kin}}+V_b \end{bmatrix} \\ &+\frac{1}{\hbar}\cdot(\Delta t)^2\cdot C_1\cdot\begin{bmatrix} 0 & -(V_a-V_b) \\ (V_a-V_b) & 0 \end{bmatrix},\end{aligned} \tag{19}$$

where

$$\begin{aligned} C_0 &= \tfrac{1}{\Delta t}\cdot\textstyle\int_{-\Delta t/2}^{\Delta t/2} f\left(t_n+\frac{\Delta t}{2}+t\right)dt, \\ C_1 &= \tfrac{1}{(\Delta t)^2}\cdot\textstyle\int_{-\Delta t/2}^{\Delta t/2} f\left(t_n+\frac{\Delta t}{2}+t\right)\cdot t\,dt. \end{aligned}$$

The integrals C_i can be evaluated analytically or by using numerical quadrature. In the latter case, the formula has to be at least fourth order accurate for C_1 and second order for C_2 in order to retain fourth order accuracy of the resulting scheme. If we want to combine the expansion with a sixth order error estimator, the accuracy of both quadrature formulae has to be increased by two orders.

Note that using only the first term in $\Omega^{[4]}(t_{n+1},t_n)$ yields a second order accurate propagator. Also note that the second term has an appealing form, since no kinetic energy matrix is involved. This means that no furher FFT/IFFT computations are required when this term is added, and the fourth order scheme is only

marginally more computationally demanding than the second order method. However, higher order terms in the Magnus expansion are still quite complicated and involve commutators of kinetic and potential energies. For a sixth order propagator, the following term needs to be added [19]:

$$
\begin{aligned}
\tilde{\theta}_3 = &-\mathrm{i}\frac{6}{5}C_1^2(\Delta t)^3\begin{pmatrix} \Delta V & 0 \\ 0 & \Delta V \end{pmatrix} \\
&-\mathrm{i}\frac{1}{2}\left(C_2 - \frac{C_0}{12}\right)(\Delta t)^3\begin{pmatrix} -2C_0\Delta V & -(\Delta V)^2 + [T_{\mathrm{kin}}, \Delta V] \\ -(\Delta V)^2 - [T_{\mathrm{kin}}, \Delta V] & 2C_0\Delta V \end{pmatrix} \\
&-\frac{1}{60}C_1(\Delta t)^4 \times \\
&\begin{pmatrix} -4C_0[T_{\mathrm{kin}}, \Delta V] \\ -4C_0^2\Delta V - (\Delta V)^3 - [T_{\mathrm{kin}}, [T_{\mathrm{kin}}, \Delta V] + (\Delta V)^2] - V_b[T_{\mathrm{kin}}, \Delta V] + [T_{\mathrm{kin}}, \Delta V]V_a \\ 4C_0^2\Delta V + (\Delta V)^3 + [T_{\mathrm{kin}}, [T_{\mathrm{kin}}, \Delta V] - (\Delta V)^2] + V_a[T_{\mathrm{kin}}, \Delta V] - [T_{\mathrm{kin}}, \Delta V]V_b \\ 4C_0[T_{\mathrm{kin}}, \Delta V] \end{pmatrix},
\end{aligned}
$$

where $\Delta V = V_e - V_g$ and

$$C_2 \quad = \tfrac{1}{(\Delta t)^3} \cdot \textstyle\int_{-\Delta t/2}^{\Delta t/2} f\left(t_n + \frac{\Delta t}{2} + t\right) \cdot t^2 \, dt.$$

Therefore, it is in general not efficient to increase the order beyond four. However, it might, e.g., be interesting to use this third Magnus term for a fourth order method with global error control. The term $\tilde{\theta}_3$ is then only required for error estimation, which is why it usually suffices to use a low order finite difference stencil for the discretization of the kinetic energy which reduces the cost of the matrix vector product to the order N. Note also that for the step size control, only one product with the matrix $\tilde{\theta}_3$ is needed compared to one for each dimension of the Krylov subspace if the sixth order approximation would actually be computed.

5.2 Comparison of different methods – Excitation of the Rb_2 molecule

We consider the excitation of Rb_2 from the $X^1\Sigma_g^+$ ground state to the $1^1\Sigma_u^+$ excited state. The data for the potential curves is taken from Park *et al.* [25]. We set the pulse width to 100 fs, the wavelength $\lambda = 1000$ nm, and E_0 =21.9 cm^{-1}. The system evolves over 340 fs on a spatial grid with 256 points.

In the tables describing the computational efficiency below, we use the notation $n_1(n_2)$ to refer to the adaptive Magnus–Lanczos method of order n_1 using the term $\tilde{\theta}_{n_2-1}$ for error control. Also, the notation n_1/fixed referes to a the n_1th order Magnus–Lanczos method using a fixed time step.

The three first rows of Table 1 compare the performance of the different versions of the adaptive algorithm. The methods 2(4) and 4(4) both use an approximation of the error of the second order method to choose the step size. Since including also the second term in Eq. (19) does not require any additional FFT computations, the cost per time step for the 2(4) and 4(4) methods are very similar. However, the 4(4) method produces a slighly more accurate solution.

If we are interested in meeting a certain global accuracy criterion, the Magnus term $\tilde{\theta}_3$ could be used to estimate the error for the fourth order scheme. Since this term is relatively complicated, each time step of the 4(6) scheme is considerably more expensive than for 4(4), even if no additional FFT/IFFT computations are involved (cf. the discussion in the last paragraph of Sec. 5.1). However, as is clear from Table 1, the 4(6) method

method	no. steps	no. FFT/IFFT	ℓ_2 error	ℓ_2 error $1^1\Sigma_u^+$ state
2(4)	24481	$74480 \cdot 2$	$1.7 \cdot 10^{-6}$	$1.2 \cdot 10^{-6}$
4(4)	24487	$74468 \cdot 2$	$9.4 \cdot 10^{-7}$	$1.8 \cdot 10^{-7}$
4(6)	906	$4530 \cdot 2$	$8.8 \cdot 10^{-6}$	$6.2 \cdot 10^{-6}$
2/fixed	24481	$69040 \cdot 2$	$6.2 \cdot 10^{-6}$	$6.0 \cdot 10^{-6}$
2/fixed	49500	$136243 \cdot 2$	$1.7 \cdot 10^{-6}$	$1.6 \cdot 10^{-6}$
4/fixed	906	$4516 \cdot 2$	$5.5 \cdot 10^{-5}$	$5.2 \cdot 10^{-5}$
4/fixed	1439	$6828 \cdot 2$	$8.8 \cdot 10^{-6}$	$8.2 \cdot 10^{-6}$

Table 1: Different kinds of error control with tolerance 10^{-5}.

is still much more efficient than if the less accurate error estimator is used. The number of time steps can be reduced by a factor of 27 and the number of FFT/IFFT pairs, i.e. the work, with a factor of 17 compared to method 2(4).

In the last column of Table 1, we report the ℓ_2 error of the excited state function only. In a practial computation, the excited state wave function is often the interesting part of the result. We note that the error is mostly concentrated in the excited state, and the error estimator used (which is defined for the full wavefunction) is still efficient.

In order to show the efficiency gain of the adaptive method, we also show results for fixed step schemes in Table 1. For example, we take the number of iterations needed by the 4(6) method and compute the solution with the same number of steps but fixed step length. This results in a significantly larger error using just a slightly smaller number of FFT/IFFT evaluations compared to the adaptive scheme. From the results in the table, we also observe that the fixed step algorithm needs more than one and a half times as many steps to reach the same accuracy as the adaptive variant. Correspondingly, for the second order Magnus–Lanczos scheme with a fixed time step we need about twice as many steps to reach the same accuracy as the 2(4) adaptive method.

5.3 A problem with several spatial degrees of freedom — Excitation of the ClO_2 molecule

To demonstrate that the new propagators are applicable also to problems with several spatial degrees of freedom, we consider a model of the chlorine-dioxid molecule [1, 36, 31] which involves three degrees of freedom. We propagate the solution over 60 fs with a laser of strength 21.9 cm^{-1}, wavelength 386 nm, and width 20 fs. We use Radau coordinates with a computational grid of size 128 x 128 x 64 and use potential energy surfaces due to [27]. The results are summarized in Table 2. Again, our adaptive algorithm gives an effective error bound and we need almost 50% more FFT computation to reach the same accuracy with an equidistant grid.

5.4 A problem with a transparent boundary condition and three states — Dissociation of the IBr molecule

We have also applied our new propagation algorithms to a model of a IBr system. As for the Rb_2 model studied earlier, the problem is one-dimensional. However, for the

method	no. steps	no. FFT/IFFT	ℓ_2 error
2(4)	3034	$14799 \cdot 2$	$3.6 \cdot 10^{-5}$
2/fix	3034	$13827 \cdot 2$	$4.3 \cdot 10^{-5}$
2/fix	5000	$21114 \cdot 2$	$3.6 \cdot 10^{-5}$

Table 2: OClO with tolerance 10^{-4} (3D).

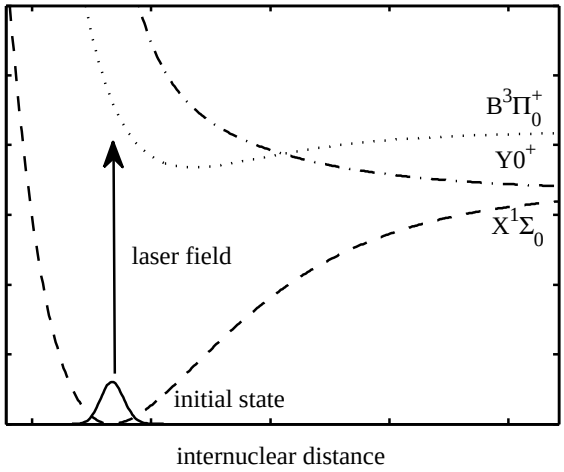

Figure 2: Configuration of the IBr system with three electronic states.

IBr example a third, dissociative state is included. Note that the Magnus–Lanczos algorithm developed in Sec. 3 can be applied also for dissociative problems, provided that the Lanczos algorithm is replaced by the Arnoldi iteration [29]. The computations presented below are performed using such a Magnus-Arnoldi scheme.

Starting with the lowest eigenfunction of the ground state, we excite the IBr molecule to the $B^3\Pi_0^+$ state with a laser with a wavelength of 500nm, a width of 50fs and strength 219 cm^{-1}. This state is statically coupled to the $Y0^+$ dissociative state. For the parameters of the potential energy curves, we refer to [10]. Fig. 2 shows the configuration in this system and Fig. 3 visualizes the evolution of the wave packet in the three states. The latter figure also includes the corresponding potential energy surfaces. One can see that the wave packet stays stable in the ground state, whereas the fraction that is excited moves away from the origin.

The spatial coordinate is discretized with 419 grid points and an complex absorbing potential (CAP) boundary of the form described by Grozdanov and McCarroll [9] is introduced at the last 82 points. The CAP-parameters are chosen such that the reflections from the sponge layer are negligible compared to the propagation error. The first Magnus-terms for a three-state system are described in detail in [19].

Table 3 shows the results for a propagation over 120 fs. Apart from the ℓ_2 error, we also consider the error in the cross-correlation with the 14th eigenstate of the B_0^+ state. This

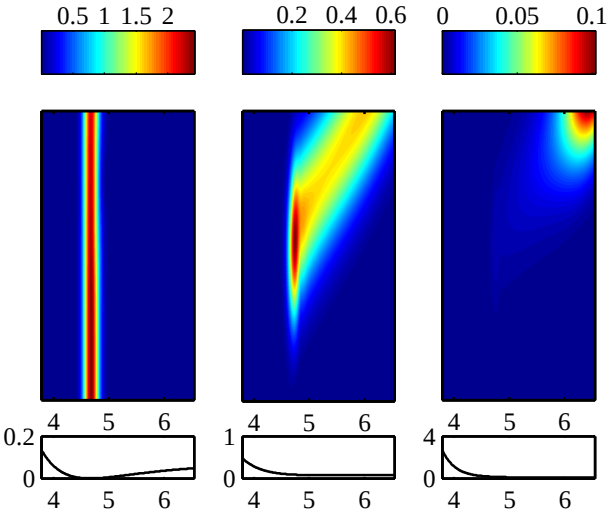

Figure 3: Time-evolution of the IBr system. In the lower row, the potential energies are shown (from left to right; $X^1\Sigma_0$, $B^3\Pi_0^+$, $Y0^+$). Above each potential, the evolution of the corresponding wave packet is visualized (time axis from bottom to top, internuclear distance from left to right).

method	no. steps	no. FFT/IFFT needed	ℓ_2 error
2(4)	4504	$21614 \cdot 3$	$1.6 \cdot 10^{-4}$
2/fix	4504	$21929 \cdot 3$	$3.4 \cdot 10^{-4}$
2/fix	6600	$29903 \cdot 3$	$1.6 \cdot 10^{-4}$

Table 3: IBr with tolerance 10^{-3} (including dissociation).

is the highest eigenstate with energy below the energy crossing with the Y_0^+ state. For our adaptive computations, we get an absolute error of $6.5 \cdot 10^{-8}$. This means that the error is significantly overestimated for this functional. However, considering that the cross-correlation itself is of size $6.0 \cdot 10^{-6}$, we end up with an relative error of $1.1 \cdot 10^{-2}$ which is above the tolerance. The reason for this beahviour is that the main part of the error in concentrated in the excited states, an observation which is further discussed in Sec. 6 below. Note that our error estimator considers the absolute error and, thus, cannot make a rigorous prediction for the relative error.

6 Efficiency of the Low-Cost Error Estimate contra the Costs of Solving the Dual Problem

For the TDSE, the absolute value of the dual solution is known in advance, and we exploit this fact to derive the global error estimate (4). However, in Eq. (3), the absolute value as well as the direction of the dual solution provide information on the size of the error. Note that Cao and Petzold [5] consider a single ODE where the direction is reduced to the sign of the solution. Hence, by taking the norm we loose the information of the direction which potentially makes the estimate less efficient for error control. On the other hand, the estimate is available from only solving the primal problem once which reduced the computational cost significantly compared to if a general method for error control is used. Also, in case the functional $\langle z, \cdot \rangle$ depends on the error, using (4) is often advantageous since the vector z is unknown.

In case one wants to include the directional information of the dual solution, the following adaptive procedure would be suggested:

- Solve the dual solution with low tolerance and save it for each time step
- Solve the primal solution with adaptively choosing the time step according to

$$k_i = \left(k_{i-1} \frac{\varepsilon / T}{\langle \lambda(t_i), \widetilde{\Omega}^{[2n+2]}(t_i, k_{i-1})) \widetilde{\psi}(t_i) \rangle} \right)^{\frac{1}{2n}} \cdot k_{i-1}, \tag{20}$$

  where $\lambda(t_i)$ can be estimated by linear interpolation of the precomputed values

Note that this algorithm is generally not practical since it requires too much memory for saving the dual solution at every time step. For the case with a symmetric Hamiltonian, this can be solved by exploiting the time-reversibility of the Schrödinger equation: Solve the dual problem first without saving, then use the solution at initial time as initial value for a forward problem on the same discrete time points and solve this problem parallely with the primal problem. For dissociative states one has to work with reversal schedules [34].

As a specific example of the effect of using our low-cost error estimator, we revisit the Rb_2 model studied in Sec. 5.2. For the computations performed there, we used that the norm of the dual solution is constant and did not actually compute it. For comparison, we have also solved the problem adaptively based on (20), i.e., including a computation of the dual solution. We consider the error in the auto-correlation function (cross-correlation with the initial state) as well as the error in the cross-correlation function with the lowest eigenstate on the excited state. In both cases, we precompute the dual solution with 5000 time steps (equidistant).

For the auto-correlation, we now find that 8083 (+129 disapproved) steps are needed and for the cross-correlation, we need 24252 steps. In the first case, the number of steps can be reduced by a large amount by solving the dual problem as well, whereas one almost needs as many steps as without solving the dual problem when focusing on the cross-correlation function. This verifies the earlier observation that the error is concentrated on the excited state, considering that the auto-correlation takes a value of $-(0.03+0.10\mathrm{i})$ and the cross-correlation a value of $-(0.52+0.85\mathrm{i})$. We observe that while the total computing costs decrease when explicitly soving the dual equation in the first case, they increase in the second.

One specific problem setting which requires special attention is if we want to compute a cross-correlation function which is small. In this case, the overestimation provided by our low-cost error estimator might not be acceptable (cf. Sec. 5.4). Then, we have to trade the efficiency of the estimator against the cost of solving the equation several times. Which way to choose is, of course, problem dependent (cf. the discussion in the last paragraph of Sec. 5.4).

Here, it should be noted that when discussing the error in the computation of a small cross-correlation, it makes no sense to consider the absolute error. If one assumes the error to be directed in the same direction as the solution, the standard procedure yields an estimate for the relative error. But in practice, we have to be aware that we do not have a strict bound on the relative error since the direction of the solution is only a rough approximation for the direction of the error.

Indeed, we found in our experiments that the part of the error in the excited state is usually much larger than the excited-state-part of the solution. This seems reasonable since the initial state was an eigenfunction of the ground state Hamiltonian. Therefore, the wave function in the ground state to a main extent remains within this eigenstate. It then changes slowly compare to the excited state wave function and is hence relatively easy to approximate.

To sum up, it pays off computing the dual solution if

- there is a functional of the error we are especially interested in and
  - the value of the functional is very small compare to the norm of the wave function or
  - the error is concentrated away from the interesting functional,
- and we have enough memory accessible to save the dual solution on a coarse grid or we have an efficient scheme to compute the dual solution parallely with the primal.

7 Summary and Conclusions

We have proposed and analyzed an h,p-adaptive propagator for the time-dependent Schrödinger equation that allows for a global error control. The local error is estimated based on extrapolation at the cost of effectively one (sparse) matrix-vector multiplication for a second order propagator. Duality-based error estimation theory was applied to investigate the influence of local errors on the result at some final time T. As long as no sponge layer is involved, the time-dependent Schrödinger equation has a special structure making the primal and the dual PDE the same. Using furthermore the fact that the norm is conserved, we get the global estimate without solving the dual problem.

In this article, we focused on time-discretization techniques and used a simple FFT implementation of a pseudo-spectral method for space discretization. In order to make this method competitive especially for higher dimensions, it has to be combined with adaptivity in space in future work.

References

[1] G. Barinovs, N. Marković, and G. Nyman. Split operator method in hyperspherical coordinates: Application to CH_2I_2 and OClO. *J. Chem. Phys.*, 111:6705–6711Univ, 1999.

[2] R. Becker and R. Rannacher. An optimal control approach to a posteriori error estimation in finite element methods. *Acta Numerica*, pages 1–102, 2001.

[3] S. Blanes, F. Casas, and J. Ros. Improved high order integrators based on the Magnus expansion. *BIT Numer. Math.*, 40:434–450, 2000.

[4] S. Blanes and P. C. Moan. Fourth- and sixth-order commutator-free Magnus integrators for linear and non-linear dynamical systems. *Appl. Numer. Math.*, 56:1519–1537, 2006.

[5] Y. Cao and L. Petzold. A posteriori error estimate and global error control for ordinary differential equations by the adjoint method. *SIAM J. Sci. Compt.*, 26:359–374, 2004.

[6] K. Eriksson, C. Johnson, and A. Logg. Adaptive computational methods for parabolic problems. In E. Stein, R. de Borst, and T. J. R. Hughes, editors, *Encyclopedia of Computational Mechanics*, pages 36–61. John Wiley & Sons, 2004.

[7] C. W. Gear. *Numerical Initial Value Problems in Ordinary Differential Equations*. Prentice-Hall, Englewood Cliffs,NJ, 1971.

[8] S. K. Gray and J. M. Verosky. Classical Hamiltonian structures in wave packet dynamics. *J. Chem. Phys.*, 100:5011–5022, 1994.

[9] T. P. Grozdanov and R. McCarroll. Multichannel scattering calculations using absorbing potentials and mapped grids. *J. Chem. Phys.*, 126:034310, 2007.

[10] H. Guo. The effect of nonadiabatic coupling in the predissociation dynamics of IBr. *J. Chem. Phys.*, 99:1685–1692, 1993.

[11] T. Hagstrom. New results on absorbing layers and radiation boundary conditions. In M. Ainsworth, P. Davies, D. Duncan, P. Martin, and B. Rynne, editors, *Topics in Computational Wave Propagation*, pages 1–42. Springer, Berlin, 2003.

[12] E. Hairer, S. P. Nørsett, and G. Wanner. *Solving Ordinary Differential Equations I, Nonstiff Problems*. Springer, Berlin, 1993.

[13] S. Hein, T. Hohage, and W. Koch. On resonances in open systems. *J. Fluid Mech.*, 506:255–284, 2004.

[14] M. Hochbruck and C. Lubich. On Magnus integrators for time-dependent Schrödinger equations. *SIAM J. Numer. Anal.*, 41:945–963, 2003.

[15] M. Hochbruck, C. Lubich, and H. Selhofer. Exponential integrators for large systems of differential equations. *SIAM J. Sci. Compt.*, 19:1552–1574, 1998.

[16] S. Holmgren, C. Peterson, and H. O. Karlsson. Time-marching methods for the time-dependent Schrödinger equation. In *Proc. of the International Conference on Computational and Mathematical Methods in Science and Engineering*, pages 53–56, 2004.

[17] A. Iserles, H. Z. Munthe-Kaas, S. P. Nørsett, and A. Zanna. Lie-group methods. *Acta Numerica*, 9:215–365, 2000.

[18] C. S. Kenney and A. J. Laub. Small-sample statistical condition estimates for general matrix functions. *SIAM J. Sci. Comput.*, 15:36–61, 1994.

[19] K. Kormann, S. Holmgren, and H. O. Karlsson. Accurate time-propagation of the Schrödinger equation with an explicitly time-dependent Hamiltonian. *J. Chem. Phys.*, 128:184101, 2008.

[20] C. Leforestier, R. H. Bisseling, C. Cerjan, M. D. Feit, R. Friesner, A. Guldberg, A. Hammerich, G. Jolicard, W. Karrlein, H.-D. Meyer, N. Lipkin, O. Roncero, and R. Kosloff. A comparison of different propagation schemes for the time dependent Schrödinger equation. *J. Comput. Phys.*, 94:59–80, 1991.

[21] C. Lubich. Integrators for quantum dynamics: A numerical analyst's brief review. In J. Grotendorst, D. Marx, and A. Muramatsu, editors, *Quantum Simulation of Complex Many-Body Systems: From Theory to Algorithms*, pages 459–466. John von Neumann Institute for Computing, Julich, 2002.

[22] D. E. Manolopoulos. Derivation and reflection properties of a transmission-free absorbing potential. *J. Chem. Phys.*, 117:9552–9559, 2002.

[23] P. C. Moan and J. Niesen. Convergence of the Magnus series. *Found. Comput. Math.*, 8:291–301, 2008.

[24] A. S. Moffat. Controlling chemical reactions with laser light. *Science*, 255:1643–1644, 1992.

[25] S. J. Park, S. W. Suh, Y. S. Lee, and G.-H. Jeung. Theoretical Study of the Electronic States of the Rb_2 Molecule. *J. of Mol. Spectrosc.*, 207:129–135, 2001.

[26] T. J. Park and J. C. Light. Unitary quantum time evolution by iterative Lanczos reduction. *J. Chem. Phys.*, 85(10), 1986.

[27] K. A. Peterson. Accurate ab initio near-equilibrium potential energy and dipole moment functions of the X^2B_1 and first excited $^1A_2$ electronic states of OClO and OBrO. *J. Chem. Phys.*, 109:8864–8875, 1998.

[28] A. D. Raptis and J. R. Cash. A variable step method for the numerical integration of the one-dimentional Schrödinger equation. *Computer Physics Communications*, 36:113–119, 1985.

[29] Y. Saad. Analysis of some Krylov subspace approximations to the matrix exponential operator. *SIAM J. Numer. Anal.*, 29:209–228, 1992.

[30] J. M. Sanz-Serna and M. P. Calvo. *Numerical Hamiltonian Problems*. Chapman & Hall, London, 1994.

[31] Z. Sun, N. Lou, and G. Nyman. Time-Dependent Wave Packet Split Operator Calculations on a Three-Dimensional Fourier Grid in Radau Coordinates Applied to the OClO Photoelectron Spectrum. *J. Phys. Chem. A*, 108:9226–9232, 2004.

[32] D. J. Tannor. *Introduction to Quantum Mechanics: A Time-Dependent Perspective*. University Science Books, Sausalito, 2007.

[33] D. J. Tannor and S. A. Rice. Control of selectivity of chemical reaction via control of wavepacket evolution. *J. Chem. Phys.*, 83:5013 – 5018, 1985.

[34] A. Walther. *Program Reversal Schedules for Single and Multi-processor Maschines*. PhD thesis, Institute of Scientific Computing, TU Dresden, 1999.

[35] J. Wensch, M. Däne, W. Hergert, and A. Ernst. The solution of strationary ODE problems in quantum mechanics by Magnus methods with stepsize control. *Comput. Phys. Commun.*, 160:129–139, 2004.

[36] K.-J. Yuan, Z. Sun, S.-L. Cong, and N. Lou. Selective excitation of the OClO molecule with femtosecond laser pulse. *Phys. Rev. A*, 72:052513, 2005.

[37] A. H. Zewail. *Femtochemistry: Ultrafast Dynamics of the Chemical Bond*. World Scientific, World Scientific, 1994.